

Oscillation-Independent Probes of Neutrino Non-Standard Interactions from Supernovae

ANGELA R. BEATTY,^{1,2,*} ANNA M. SULIGA ,^{3,†} AND VOLODYMYR TAKHISTOV ,^{4,5,6,7,‡}

¹*Department of Physics and Astronomy, San Francisco State University, 1600 Holloway Ave, San Francisco, 94132, California, USA*

²*Department of Physics, University of California Berkeley, Berkeley, California 94720, USA*

³*Center for Cosmology and Particle Physics, New York University, New York, NY 10003, USA*

⁴*International Center for Quantum-field Measurement Systems for Studies of the Universe and Particles (QUP, WPI), High Energy Accelerator Research Organization (KEK), Oho 1-1, Tsukuba, Ibaraki 305-0801, Japan*

⁵*Theory Center, Institute of Particle and Nuclear Studies (IPNS), High Energy Accelerator Research Organization (KEK), Tsukuba 305-0801, Japan*

⁶*Graduate University for Advanced Studies (SOKENDAI), 1-1 Oho, Tsukuba, Ibaraki 305-0801, Japan*

⁷*Kavli Institute for the Physics and Mathematics of the Universe (WPI), UTIAS, The University of Tokyo, Kashiwa, Chiba 277-8583, Japan*

ABSTRACT

We introduce the first oscillation-independent astrophysical method to probe non-standard neutrino interactions (NSI) in core-collapse supernovae. Using a self-consistent treatment of NSI effects in both supernova neutrino emission simulations and flavor independent neutral-current scattering in detectors, we show that anti-correlated coincidence signatures between liquid scintillator experiments such as JUNO and dark matter detectors such as DARWIN/XLZD, ARGO, or RES-NOVA break degeneracy between NSI and flavor conversions effects. For a Galactic supernova within $\lesssim 1$ kpc this approach enables independent probes of neutrino-quark NSI couplings in parameter space overlapping and extending beyond existing terrestrial limits. Our results establish a novel oscillation-independent avenue to test fundamental neutrino interactions in extreme astrophysical environments.

1. INTRODUCTION

The detection of neutrinos from supernova 1987A (Hirata et al. 1987; Bionta et al. 1987; Alexeyev et al. 1988) established multi-messenger astronomy of transient events. While only a handful of $\bar{\nu}_e$ were observed, the subsequent discovery of neutrino masses through observation of neutrino oscillations effects in solar and atmospheric neutrino fluxes (Fukuda et al. 1998; Ahmad et al. 2002) demonstrated physics beyond the Standard Model (SM) in the neutrino sector. New fundamental “non-standard neutrino interactions” (NSI) with matter (Wolfenstein 1978; Valle 1987; Dev et al. 2019) arise in many theories and can strongly affect neutrinos in CCSNe (Nunokawa et al. 1996; Lei et al. 2020; Mikheyev & Smirnov 1985; Mansour & Kuo 1998; Fogli et al. 2002; Esteban-Pretel et al. 2010; Blennow et al. 2008; Stapleford et al. 2016; Farzan et al. 2018; Suliga & Tamborra 2021; Cerdeño et al. 2021, 2023; Dutta et al. 2025). Terrestrial probes constrain neutrino-quark NSI primarily through their effects on the neutrino oscillations (e.g. (Weatherly et al. 2022)) or coherent elastic nucleus-neutrino scattering (Aki-

mov et al. 2017, 2021; Aprile et al. 2021; Bonet et al. 2022; Adamski et al. 2025).

The extreme conditions of CCSN comprising dense, hot and degenerate environment constitute an ideal laboratory for probing fundamental neutrino properties. Neutrino-quark NSI can strongly affect CCSN emission during the pre-neutronization phase preceding the neutronization burst (Huang et al. 2021). Within $\lesssim 1$ kpc over 30 candidates that could undergo core-collapse in the next few decades have already been identified (Mukhopadhyay et al. 2020). Among the closest is Betelgeuse (α -Ori), with mass 16.5–19 M_\odot and distance 168^{+27}_{-15} pc (Joyce et al. 2020). Detecting this early “pre-SN” neutrino signal is of particular interest, and a dedicated early-warning system has recently been implemented by Super-Kamiokande and KamLAND (Abe et al. 2024).

In this work we introduce the first astrophysical method to probe NSI independently of flavor conversions in CCSN using neutral-current (NC) coincidence signatures across pairs of detectors. Distinct flavor independent NC channels, exhibiting opposite responses in different experiments, produce anti-correlated signatures that break cross section and luminosity degeneracies limiting single-channel studies. We demonstrate this with self-consistent CCSN simulations that incorporate NSI effects on neutrino opacities in the proto-

* abeatty@sfsu.edu

† a.suliga@nyu.edu

‡ vtakhist@post.kek.jp

neutron star and propagate the resulting fluxes to predict observable signatures in terrestrial detectors.

2. NON-STANDARD NEUTRINO INTERACTIONS

We consider vector NC neutrino NSI generated by a heavy mediator, described by the effective four-fermion interaction Lagrangian (Wolfenstein 1978; Dev et al. 2019)

$$\mathcal{L}_{\text{NSI}} = -2\sqrt{2}G_F \epsilon_{\alpha\beta}^{fV} (\bar{\nu}_{\alpha L} \gamma^\rho \nu_{\beta L}) (\bar{f} \gamma_\rho f), \quad (1)$$

where $G_F = 1.1664 \times 10^{-5}$ GeV $^{-2}$ is the Fermi constant, $\alpha, \beta = e, \mu, \tau$ represent neutrino flavors, and $f = u, d$ are the quark fields. Here, we consider NSI interactions exclusively with first generation quarks. Further, we focus on flavor-conserving diagonal NSI, with $\alpha = \beta$, interacting with all neutrino flavors ν_e , ν_μ and ν_τ . With the NSI couplings between neutrinos and quarks $\epsilon^{u(d)V} = \epsilon_{ee}^{u(d)V} = \epsilon_{\mu\mu}^{u(d)V} = \epsilon_{\tau\tau}^{u(d)V}$.

We implement NSI effects on interaction cross sections assuming that only one quark coupling is nonzero at a time, if $\epsilon^u \neq 0$ then $\epsilon^d = 0$, and vice versa. Since we consider flavor-universal diagonal NSI couplings, therefore we do not anticipate to modify Mikheyev-Smirnov-Wolfenstein (Wolfenstein 1978; Mikheev & Smirnov 1986) flavor conversion probabilities inside CCSN. In addition, constraints from existing terrestrial oscillation experiments (e.g. (Weatherly et al. 2022)) do not directly apply.

2.1. Neutral Current Channels

In the following we focus on NC neutrino interactions and examine the impact of NSI on both coherent elastic neutrino-nucleus scattering (CE ν NS) and elastic neutrino-proton scattering. The differential CE ν NS cross section for $X(A, Z) + \nu \rightarrow X(A, Z) + \nu$ in the SM is (Freedman 1974)

$$\frac{d\sigma_{\nu X}}{dE_r} \simeq \frac{G_F^2 m_X}{4\pi} Q_W^2 \left(1 - \frac{m_X E_r}{2E_\nu^2}\right) F^2(Q), \quad (2)$$

where E_ν is the incoming neutrino energy, heavy nucleus $X(A, Z)$ mass is $m_X \simeq 931.5A$ MeV with A , and Z being respectively the nucleus mass and atomic numbers, $Q_W = [N - Z(1 - 4\sin^2(\theta_W))]$ is the SM weak charge, $\sin^2 \theta_W = 0.23863$ is the weak mixing angle at low momentum transfer (Workman et al. 2022), N is the neutron number and E_r is the nuclear recoil energy. For low momentum transfer the scattering is fully coherent with $F(Q) \simeq 1$, while at higher $Q = \sqrt{2m_X E_r}$ finite-size effects need to be included. We adopt the Helm form factor (Helm 1956)

$$F(Q) = 3 \frac{j_1(QR_0)}{QR_0} \exp\left(-\frac{1}{2}Q^2 s^2\right), \quad (3)$$

where j_1 is a spherical Bessel function of the first kind, the size of the nucleus is taken to be $R_0 = \sqrt{R^2 - 5s^2}$ with

$R = 1.2A^{\frac{1}{3}}$ fm and we assume that the nuclear skin thickness $s \simeq 0.5$ fm.

The presence of NSI modifies the CE ν NS cross section through the weak charge, which for NSI takes the form $Q_W^{\text{NSI}} = -2 [Z(2\epsilon^u + \epsilon^d) + N(\epsilon^u + 2\epsilon^d)]$. This gives an effective charge of $Q'_W = Q_W + Q_W^{\text{NSI}}$. The corresponding cross section $\sigma_{\nu X}^{\text{NSI}}$ is then obtained by replacing Q_W with Q'_W in Eq. (2). The ratio of modified by NSI and unmodified SM cross sections is then $\sigma_{\nu X}^{\text{NSI}}/\sigma_{\nu X}^{\text{SM}} = Q'_W/Q_W^2$.

The SM neutrino-proton elastic scattering ν -p cross section for SN neutrino energies is given by (Beacom et al. 2002; Dasgupta & Beacom 2011)

$$\frac{d\sigma_{\nu p}}{dE_p} \simeq \frac{G_F^2 m_p^2}{2\pi E_\nu^2} (BE_\nu^2 + C(E_\nu - E_p)^2 + Dm_p E_p), \quad (4)$$

where E_p is the proton recoil energy, m_p the proton mass, and the coefficients are $B = (c_V + c_A)^2$, $C = (c_V - c_A)^2$, and $D = (c_V^2 + c_A^2)$ with $c_V \simeq 0.02$, $c_A = 1.27/2$ for neutrinos and $c_A = -1.27/2$ for antineutrinos. The modification to the SM $\sigma_{\nu p}$ cross section due to vector NSI can be accounted for by replacing c_V with $c'_V = c_V + 2\epsilon^u + \epsilon^d$. Unlike CE ν NS, however, the ratio of the NSI-modified and the unmodified SM cross sections for ν -p scattering is energy dependent.

Additional NC channels can also complement our analysis. In water Cherenkov detectors inelastic neutrino scattering on ^{16}O produces de-excitation γ -rays below 10 MeV and has been proposed as a probe of SN ν_μ and ν_τ fluxes (Langanke et al. 1996). Although this signal is obscured by the inverse beta decay background, neutron tagging with gadolinium in Super-Kamiokande (Abe et al. 2022) can facilitate post-processing analyses to identify it. Further, potentially promising NC channels from ^{40}Ar targets in liquid argon time projection chamber DUNE detector (Abi et al. 2021) have been put forth (Tornow et al. 2022; Newmark & Schneider 2023).

3. SUPERNOVA NEUTRINO EMISSION

The standard scenario of the CCSN begins with the infall phase, when the inner core approaches the Chandrasekhar mass and electron degeneracy pressure can no longer provide support against gravity. Rapid collapse leads to enhanced electron neutrino emission primarily from electron captures on nuclei. Once the density reaches approximately few $\times 10^{11}$ g cm $^{-3}$, the neutrino diffusion timescale exceeds the collapse timescale, and neutrinos become trapped through frequent direction-changing scattering off nuclei. This results in a distinct pre-neutronization peak in the neutrino emission signal.

To analyze the impact of NSI on SN neutrino emission, we model the neutrino signal using the 1D CCSN simulation code GR1D (O’Connor & Ott 2010; O’Connor 2015) together

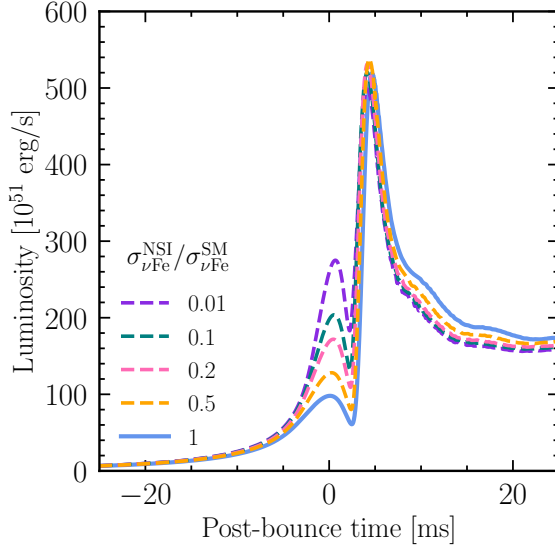


Figure 1. All-flavor neutrino luminosity in the observer frame as a function of post-bounce time from our one-dimensional GR1D CCSN simulations with (dashed) and without (solid blue) NSI. The NSI effects correspond to $\epsilon^u < 0.16$, where there is a negative interference with the SM contribution for CE ν NS, while the solid line represents the SM case with $\epsilon^u = 0$ and $\sigma_{\nu \text{Fe}}^{\text{NSI}}/\sigma_{\nu \text{Fe}}^{\text{SM}} = 1$.

with NuLib code (Sullivan et al. 2016) for neutrino opacities. For both the SM and NSI scenarios we include the dominant neutrino-nucleus processes, which are electron captures on nuclei and nucleons as well as CE ν NS. We adopt a $15 M_\odot$ progenitor with solar metallicity (Woosley & Weaver 1995) as our benchmark model. Throughout, we use the output luminosity of non-electron neutrinos from the simulation as the sum of all four species ν_μ , ν_τ , $\bar{\nu}_\mu$, and $\bar{\nu}_\tau$.

Modifications from NSI to the CE ν NS cross section can significantly alter the shape of the CCSN pre-neutronization neutrino peak (Huang et al. 2021). We focus on NSI mediated by heavy particles with masses above a few hundred MeV. Hence, the on-shell production of such particles in the core is negligible since the temperature during infall reaches only ~ 15 MeV.

In Figure 1 we show the luminosities of all neutrino flavors from CCSN simulations with and without NSI effects. During the pre-neutronization burst the luminosity increases in the NSI case compared to SM interactions only. The luminosity increase originates from a significantly smaller CE ν NS cross-section when NSI are present and the fact that heavy nuclei dominate the matter composition of the SN core during that phase (see also Figure 5). After core bounce, the luminosities in both cases become nearly identical because nucleons dominate the matter composition and NSI have a significantly smaller impact on their cross sections than for heavy nuclei (see also Appendix A Figure 4). By contrast, variations in electron capture rates in hot SN matter

can modify both the pre-burst and neutronization peaks by $\sim 20\text{--}30\%$ (Sullivan et al. 2016). These considerations highlight the need for multi-detector, multi-channel strategies to robustly identify NSI signatures.

To obtain the time-dependent neutrino flux we consider the post-bounce time (t_{pb}) luminosities $L_{\nu_\beta}(t_{\text{pb}})$, mean energies $\langle E_{\nu_\beta} \rangle$ and root-mean-squared energies $\langle E_{\nu_\beta}(t_{\text{pb}})^2 \rangle$ for each flavor $\beta = \{\nu_e, \bar{\nu}_e, 4\nu_x\}$, with $\nu_x = \{\nu_\mu, \bar{\nu}_\mu, \nu_\tau, \bar{\nu}_\tau\}$. The flavor-summed flux from CCSN at distance D is then

$$\frac{d\psi(E_\nu)}{dt_{\text{pb}}} = \sum_\beta \frac{L_{\nu_\beta}(t_{\text{pb}})}{4\pi D^2} \frac{\phi_{\nu_\beta}(E_\nu, t_{\text{pb}})}{\langle E_{\nu_\beta}(t_{\text{pb}}) \rangle}, \quad (5)$$

where E_ν is the neutrino energy. The spectral shape is approximated by a pinched distribution (Keil et al. 2003)

$$\begin{aligned} \phi_{\nu_\beta}(E_\nu, t_{\text{pb}}) &= \left(\frac{E_\nu}{\langle E_{\nu_\beta}(t_{\text{pb}}) \rangle} \right)^{\alpha_\beta(t_{\text{pb}})} \\ &\times \exp \left[-\frac{1 + \alpha_\beta(t_{\text{pb}})E_\nu}{\langle E_{\nu_\beta}(t_{\text{pb}}) \rangle} \right], \end{aligned} \quad (6)$$

where we adopt the pinching parameter $\alpha_\beta \equiv 2.3$ corresponding to Fermi-Dirac distribution. We use these fluxes to compute signal event rates in experiments.

4. EXPERIMENTAL SIGNATURES

To disentangle the effects of NSI from those of neutrino flavor conversion in the CCSN core (Duan et al. 2010; Tamborra & Shalgar 2021; Volpe 2023) we focus on NC detection channels that are to good approximation equally sensitive to all flavors. We consider signatures in both CE ν NS and elastic ν -p scattering. For CE ν NS, large scale dark matter (DM) are especially promising owing to their low thresholds, scalable volumes and heavy nuclei. The detection of CCSN neutrinos in such experiments has been extensively studied (Abe et al. 2017; Lang et al. 2016; Khaitan 2018; Kozynets et al. 2019), including sensitivity to pre-SN neutrinos (Raj et al. 2020). Low mediator mass NSI SN detection in large xenon-based DM and lead-based detectors was studied in Suliga & Tamborra (2021). In contrast, ν -p elastic scattering can be efficiently observed in liquid scintillator detectors (Beacom et al. 2002; Dasgupta & Beacom 2011), which combine sizable volumes with low energy thresholds and excellent energy resolution.

4.1. Detectors

For our analysis we consider a variety of experimental detector configurations, as described in Table 1. These follow proposals for near future experiments based on xenon such as DARWIN (Aalbers et al. 2016), which has since evolved into the XLZD concept (Aalbers et al. 2024) to which our findings also apply, based on argon such as ARGO (Aalseth et al. 2018) as well as based on lead such as RES-NOVA (Pattavina

Table 1. Number of expected detected events from Betelgeuse CCSN at $D = 0.2$ kpc up to the onset of the neutronization burst for NSI and for SM in the characteristic target detectors considered. We consider one coupling at a time with $\epsilon^u = 0.158$ ($\epsilon^d = 0$) or $\epsilon^d = 0.150$ ($\epsilon^u = 0$) resulting in the ratio for CE ν NS $\sigma_{\nu\text{Fe}}^{\text{NSI}}/\sigma_{\nu\text{Fe}}^{\text{SM}} = 0.01$. The effective volumes and energy ranges of each detector are also shown. For the calculation of the event rates in the xenon-based detectors we include the energy-dependent efficiency from XENON1T (Aprile et al. 2018). The cross section ratios refer to CE ν NS for the DM detectors (target materials xenon, lead, and argon) and ν -p elastic scattering for JUNO (target material protons).

Detector (Target)	Volume (tons)	Energy Range (keV)	$\sigma^{\text{NSI}}/\sigma^{\text{SM}}$ [$\epsilon^u = 0.158$]	$\sigma^{\text{NSI}}/\sigma^{\text{SM}}$ [$\epsilon^d = 0.150$]	$N_{\text{det}}^{\text{SM}}$	$N_{\text{det}}^{\text{NSI}}$ [$\epsilon^u = 0.158$]	$N_{\text{det}}^{\text{NSI}}$ [$\epsilon^d = 0.150$]
DARWIN (xenon)	40	1-50	0.047	0.027	151	8.8	5.06
RES-NOVA (lead)	465	1-50	0.063	0.033	22731.6	2539.8	1317.9
ARGO (argon)	300	25-1,000	0.018	0.015	104.4	1.07	0.87
JUNO (protons)	20,000	200-10,000	$\lesssim 1.15$	$\lesssim 1.05$	1802	8354	8685

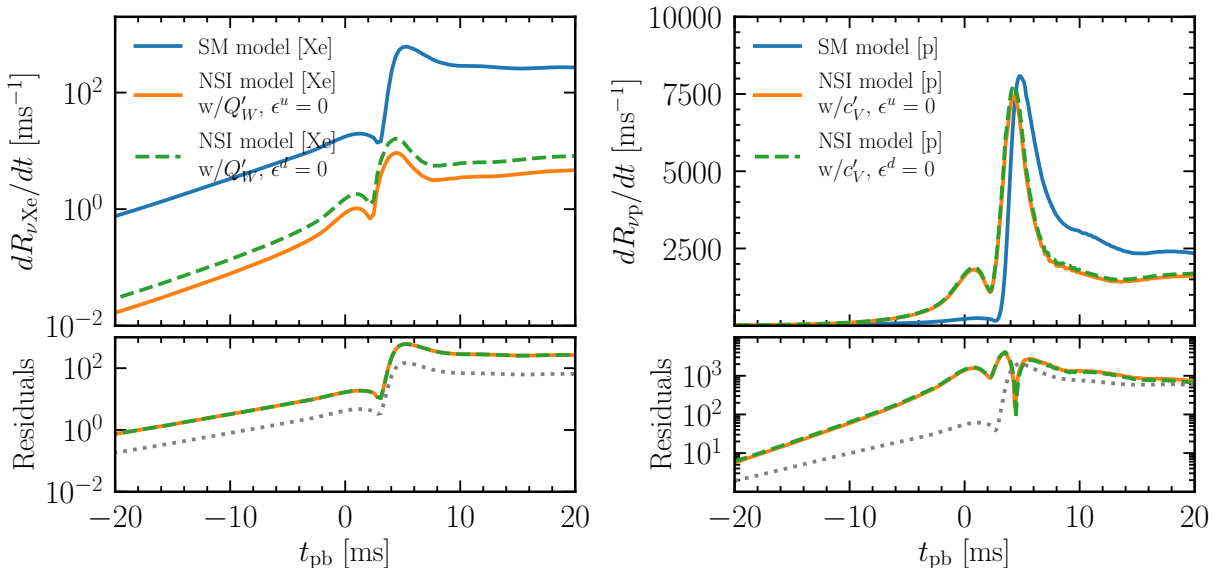


Figure 2. *Top panels:* Signal event rates for a Betelgeuse CCSN at $D = 0.2$ kpc in a xenon-based CE ν NS detector such as DARWIN (left) and a liquid-scintillator detector such as JUNO (right). The SM prediction is shown in blue, while NSI benchmarks with one coupling active at a time are shown in orange $\epsilon^d = 0.150$ ($\epsilon^u = 0$) and green $\epsilon^u = 0.158$ ($\epsilon^d = 0$), as listed in Table 1. *Bottom panels:* Residuals of the NSI event rates relative to the SM. The gray dotted line indicates a 25% uncertainty in the SM rates.

et al. 2020; Beeman et al. 2022). We consider JUNO (An et al. 2016; Lu et al. 2016) that is already operating as a representative carbon-based liquid scintillator detector.

The expected event rate in CE ν NS or ν -p elastic scattering for a given detector (det) is

$$\frac{dR_{\text{det}}}{dt_{\text{pb}} dE_r} = N_T \varepsilon(E_r) \int_{E_{\nu}^{\text{min}}}^{E_{\nu}^{\text{max}}} dE_{\nu} \frac{d\sigma_{\nu(X,p)}}{dE_r} \quad (7)$$

$$\times \frac{d\psi(E_{\nu})}{dt_{\text{pb}}} \Theta(E_r^{\text{max}} - E_r),$$

where N_T is the number of interaction targets (X nuclei type for CE ν NS or protons in the case of elastic ν -p scattering), $\varepsilon(E_r)$ is the detection efficiency and Θ is the Heaviside step function. The average energies of the CCSN neutrinos are between approximately 10-18 MeV, therefore

E_{ν}^{min} is the minimal neutrino energy to cause the recoil above observable threshold in the corresponding detector, and $E_{\nu}^{\text{max}} = 75$ MeV. The maximum recoil energy is $E_r^{\text{max}} = 2E_{\nu}^2/(m_T + 2E_{\nu})$, with $m_T = m_X$ for CE ν NS and $m_T = m_p$ for ν -p scattering. For ν -p scattering we also include the quenching of the proton recoil energy due to scattering in the scintillator medium, following Ref. (Dasgupta & Beacom 2011; An et al. 2016; Chauhan et al. 2022).

4.2. Signal Event Rates

Figure 2 shows the time dependent event rates for a Betelgeuse CCSN at $D = 0.2$ kpc in a xenon-based DARWIN detector (left) and the JUNO liquid scintillator detector (right). The upper panels compare the SM prediction (blue) with two NSI benchmarks in which only one coupling is switched on at a time: $\epsilon^u = 0.158$ ($\epsilon^d = 0$) (green, dashed) or $\epsilon^d = 0.150$ ($\epsilon^u = 0$) (orange, solid). The lower panels show the residuals of the NSI event rates relative to the SM rates. The gray dotted line indicates a 25% uncertainty in the SM rates.

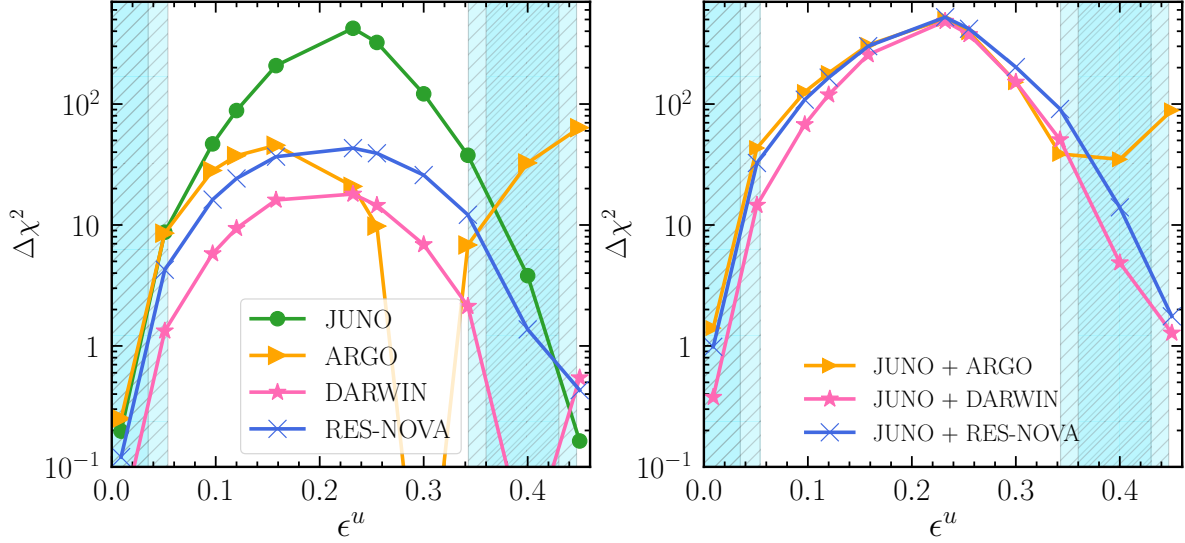


Figure 3. *Left panel:* Statistical significance ($\Delta\chi^2$) for constraining neutrino-quark NSI as a function of ϵ^u with individual detectors such as JUNO (green circles), DARWIN (pink stars), ARGO (orange triangles) and RES-NOVA (blue crosses), assuming Betelgeuse supernova at $D = 0.2$ kpc. *Right panel:* Combined $\Delta\chi^2$ for detector pairs JUNO+ARGO (orange), JUNO+DARWIN (pink), and JUNO+RES-NOVA (blue). In all cases we adopt a supernova flux normalization uncertainty $\sigma_x = 0.15$, ν -p cross section uncertainty $\sigma_y = 0.1$, and CE ν NS cross section uncertainty $\sigma_z = 0.1$. The vertical blue bands mark the 2σ (darker) and 3σ (lighter) allowed regions for $\epsilon_{\mu\mu}^u = \epsilon_{ee}^u$ from COHERENT CsI+LAr data adopted from Ref. (Coloma et al. 2022).

($\epsilon^u = 0$) (orange, solid) listed in Table 1. For CE ν NS the suppression factor $\sigma^{\text{NSI}}/\sigma^{\text{SM}}$ is fixed by the chosen ϵ and nuclear target, whereas for ν -p scattering the corresponding ratio retains neutrino energy dependence. The lower panels display the residuals of NSI rates relative to the SM.

In DARWIN the NSI event rate remains below the SM prediction. Although the neutrino luminosity during the pre-neutronization burst is nearly four times larger the CE ν NS cross section for xenon is suppressed by about a factor of twenty two. In contrast, in JUNO the NSI event rate during the burst exceeds the SM case, reflecting a small positive modification to the ν -p cross section. For the other CE ν NS detectors considered, ARGO and RES-NOVA, the NSI impact is similar to DARWIN, with consistently reduced rates (see Appendix A Figure 6).

4.3. Statistical Analysis

We evaluate the statistical significance with which a future detection of supernova neutrinos in JUNO and a large-scale DM detector could constrain the NSI parameter space. The combined sensitivity is quantified using a two-detector $\Delta\chi^2$ test statistic with Gaussian 1σ pull terms

$$\Delta\chi^2 = \min_{x,y,z} \left\{ \Delta\chi^2_{\text{JUNO}} + \Delta\chi^2_{\text{DM}} + \left(\frac{x}{\sigma_x} \right)^2 + \left(\frac{y}{\sigma_y} \right)^2 + \left(\frac{z}{\sigma_z} \right)^2 \right\}. \quad (8)$$

where we assume that $\sigma_x = 15\%$ is the supernova neutrino signal uncertainty, $\sigma_y = 10\%$ is the NC ν -p cross section

uncertainty, and $\sigma_z = 10\%$ is the CE ν NS cross section uncertainty. We minimize the statistic over the free parameters $\{x, y, z\} = (-0.99, 5]$ associated with the corresponding 1σ uncertainties.

The single detector $\Delta\chi^2_{\text{det}}$ terms are

$$\Delta\chi^2_{\text{det}} = \frac{(N_{\text{det}}^{\text{SM}}(1+x)(1+i) - N_{\text{det}}^{\text{NSI}})^2}{N_{\text{det}}^{\text{SM}}(1+x)(1+i)} \quad (9)$$

where the total number of events in a single detector $\text{det} = \{\text{JUNO}, \text{DARWIN}, \text{ARGO}, \text{RES-NOVA}\}$, with $i = y$ for JUNO and $i = z$ for the DM detectors, the total number of events in the assumed time and energy window is $N_{\text{det}}^{\text{SM}} = N_{\text{det}}(\epsilon^u = 0)$ for the SM case and $N_{\text{det}}^{\text{NSI}} = N_{\text{det}}(\epsilon^u \neq 0)$ for the NSI modified case, with the case of $\epsilon^d \neq 0$ being analogous. The total time and energy integrated number of events for a given detector is

$$N_{\text{det}} = \int_{t_0}^{t_1} dt \int_{E_r^{\text{min}}}^{E_r^{\text{max}}} dE_r \frac{dR_\nu}{dt_{\text{pb}} dE_r}, \quad (10)$$

with integration energy ranges listed in Table 1. For JUNO, the integration time extends to the dip between the pre-neutronization and neutronization bursts, while for the DM detectors we integrate to 75 ms after bounce. These assumptions yield conservative projections. Comprehensive time-dependent and energy-dependent analyses can be expected to be even more sensitive.

In the left panel of Figure 3 we show the individual detector $\Delta\chi^2$ values for JUNO, ARGO, DARWIN and RES-NOVA as a function of ϵ^u . We also display allowed regions

at 2σ and 3σ from COHERENT CsI+LAr data (Akimov et al. 2017, 2021) adopted from Ref. (Coloma et al. 2022) (see also e.g. (De Romeri et al. 2023; Liao et al. 2024)). The panel also illustrates for which values of ϵ^u the detectors with different target materials are individually not sensitive to NSI due to the degeneracy of the SM CE ν NS cross sections.

In the right panel of Figure 3 we show combined two-detector $\Delta\chi^2$ values as a function of ϵ^u for JUNO+ARGO, JUNO+DARWIN and JUNO+RES-NOVA. Our sensitivity projections from the observation of the CCSN neutrinos from Betelgeuse are excluding the same parameter space as the COHERENT CsI+LAr limits. In addition, for the combinations of JUNO+ARGO and JUNO+RES-NOVA, the region around the degenerate $\epsilon^u = 0.4$ can be excluded at more than 3σ -level. The combined $\Delta\chi^2$ are nearly always larger than the sum of the individual contributions. This reflects the anti-correlation discussed earlier, while NSI increase the signal rates in JUNO the NSI decrease signal rates in CE ν NS DM detectors for most of the considered ϵ^u values. We have also verified that increasing the distance to CCSN to 1 kpc and increasing the assumed uncertainties (see Appendix A Figure 7) do not significantly affect our conclusions.

Complementary to our analysis, DM detectors have also been identified as excellent targets for probing NSI with solar neutrinos (Harnik et al. 2012; Cerdeño et al. 2016; Böhm et al. 2019; Aristizabal Sierra et al. 2019; Suliga & Tamborra 2021; Schwemberger & Yu 2022; Schwemberger et al. 2024). Recent $> 2.5\sigma$ observations of solar neutrinos by XENONnT (Aprile et al. 2024) and PandaX-4T (Bo et al. 2024) also allow constraining NSI couplings (Aristizabal Sierra et al. 2025; Li et al. 2025; De Romeri et al. 2025; Blanco-Mas et al. 2025; Maity & Boehm 2025; Gehrlein & Kushwaha 2025) at a level comparable to the COHERENT CsI+LAr bounds already shown in Figure 3.

5. CONCLUSIONS

Using self-consistent modeling, we have demonstrated that neutrino-quark NSI can significantly alter pre-neutronization CCSN neutrino emission and result in oscillation-independent imprints in NC channels. Coincidence detection between liquid scintillator detectors such as JUNO and DM experiments such as DARWIN (and its successor concept XLZD), ARGO, or RES-NOVA exploiting the opposite NSI effects on ν -p and CE ν NS event rates provides a powerful discriminator that enables excluding regions of parameter space beyond single channel terrestrial experiment probes. Observations of a nearby Galactic supernova, within up to approximately 1 kpc, can thereby decisively test NSI couplings in the $\epsilon^u \simeq 0.035 - 0.4$ range, covering the region degenerate with the SM in terrestrial CE ν NS searches. More broadly, our results highlight that multi-detector studies of supernova neutrinos can serve as precision laboratories for fundamental neutrino interactions complementing and in some regimes surpassing terrestrial searches. Our work paves the way for future multi-experiment combined studies including detectors such as water Cherenkov Super-Kamiokande and Hyper-Kamiokande as well as liquid argon DUNE.

Acknowledgments. We thank Luca Boccioli, Peter Denton, Masayuki Nakahata, and Michael Smy for useful discussions. A.M.S. and A.R.B. acknowledge support from NSF N3AS Physics Frontier Center, NSF Grant No. PHY-2020275, and the Heising-Simons Foundation (2017-228). The work of A.M.S. is supported by the Neutrino Theory Network Program Grant DE-AC02-07CHI11359. V.T. acknowledges support by the World Premier International Research Center Initiative (WPI), MEXT, Japan and JSPS KAKENHI grant No. 23K13109. A.M.S. and V.T. also acknowledge a partial support from the Center for Theoretical Underground Physics and Related Areas (CETUP*) and its kind hospitality and stimulating research environment.

APPENDIX

A. ADDITIONAL FIGURES

Here we provide several Figures which may help to provide a deeper explanations of some of the points made in the main text of the paper.

Figure 4 shows the ratios of the NSI to SM cross sections for ^{56}Fe (solid green line), ^{131}Xe (dashed pink line), ^{40}Ar (dashed yellow line), ^{206}Pb (dashed blue line), and protons (solid and dotted purple lines). Most of the considered in our work NSI parameter space for ϵ^u results in a negative interference with the SM couplings resulting in the supersession of the CE ν NS cross sections.

The left panel of Figure 5 illustrates the changes of the temporal evolution of mean nuclear mass $\langle A \rangle$ due to the NSI in the center of the SN core for a set of SN simulations performed using GR1D (O’Connor & Ott 2010; O’Connor 2015) with the Lattimer and Sweaty equation of state (Lattimer & Sweaty 1991). The $\langle A \rangle$ tends to decrease for NSI parameters suppressing the neutrino scattering with nuclei. This effect is likely a consequence of an increased deleptonization of the SN core. The right

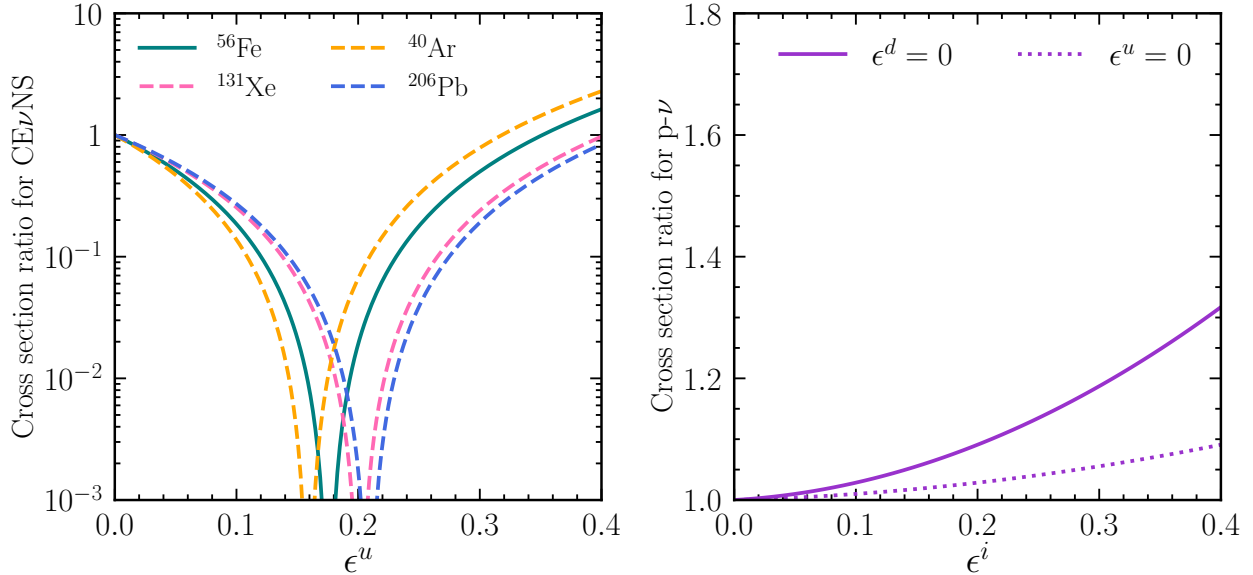


Figure 4. Ratios of the NSI cross section to the SM cross section for different elements. *Left panel:* Ratios of the CE ν NS cross sections as a function of ϵ^u for ^{56}Fe (solid green line), ^{131}Xe (dashed pink line), ^{40}Ar (dashed yellow line), ^{206}Pb (dashed blue line). *Right panel:* Ratio of the NC ν -p cross section as a function of ϵ^u (solid purple line) and ϵ^d (dotted purple line) for $E_\nu = 15$ MeV integrated over the proton recoil energy.

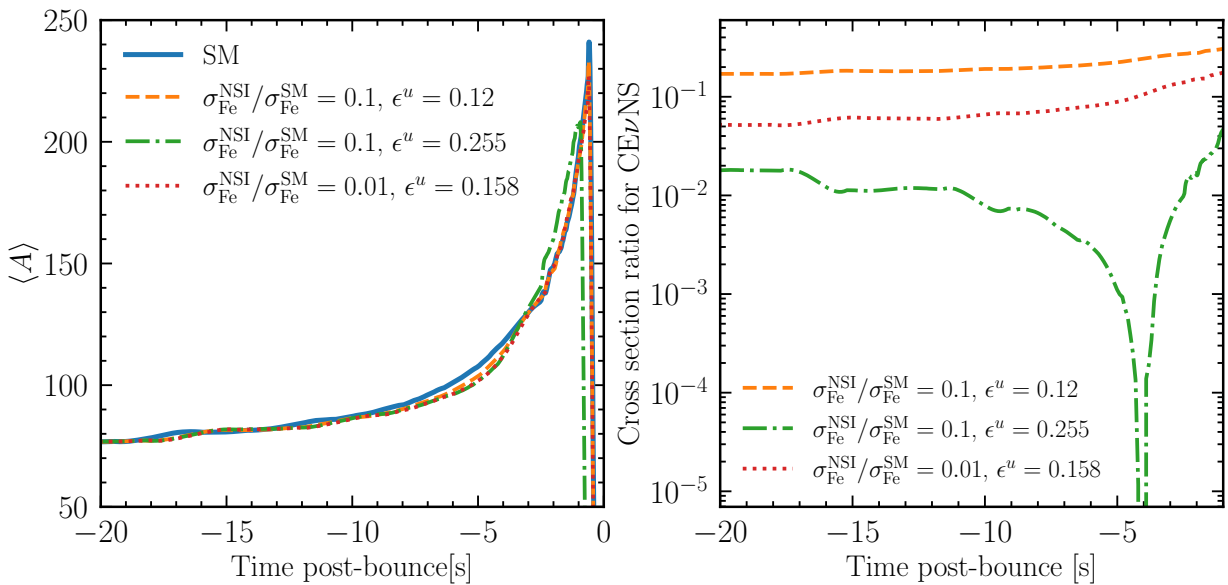


Figure 5. *Left panel:* Comparison of the evolution of the mean nuclear mass during the pre-bounce evolution simulated with the SM CE ν NS cross section (solid line) and the NSI CE ν NS cross sections (dashed lines). *Right panel:* The evolution of the ratios of the NSI to the SM cross section as a function of the post-bounce time for simulations with different values of ϵ^u .

panel of Figure 5 shows the temporal evolution of the CE ν NS cross sections ratio inside the supernova core for a set of NSI parameters.

Figure 6 shows the SM and NSI modified event rates for Betelgeuse CCSN neutrinos ($D = 0.2$ kpc) in the ARGO (left panels) and RES-NOVA (right panels) together with the residuals of the NSI rates relative to the SM in the corresponding lower panels. In the NSI case, the numerical SN simulations include the modifications to the CE ν NS and ν -p scattering with $\epsilon^u = 0.158$, resulting in the ratio for CE ν NS $\sigma_{\text{NSI}}/\sigma_{\text{SM}} = 0.01$ for ^{56}Fe . The detector characteristics used to calculate the event rates are listed in Table 1.

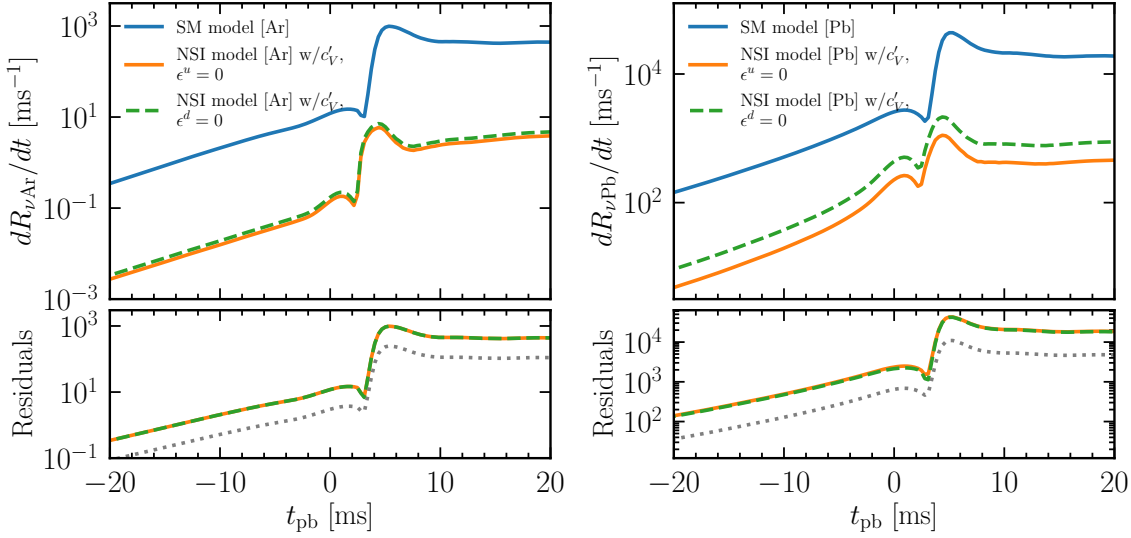


Figure 6. Same as Figure 2 but for argon-based CE ν NS detector like ARGO (left panel) and lead-based detector like RES-NOVA (right panel). The values of ϵ^u and ϵ^d used for the event rate calculations are listed in Table 1.

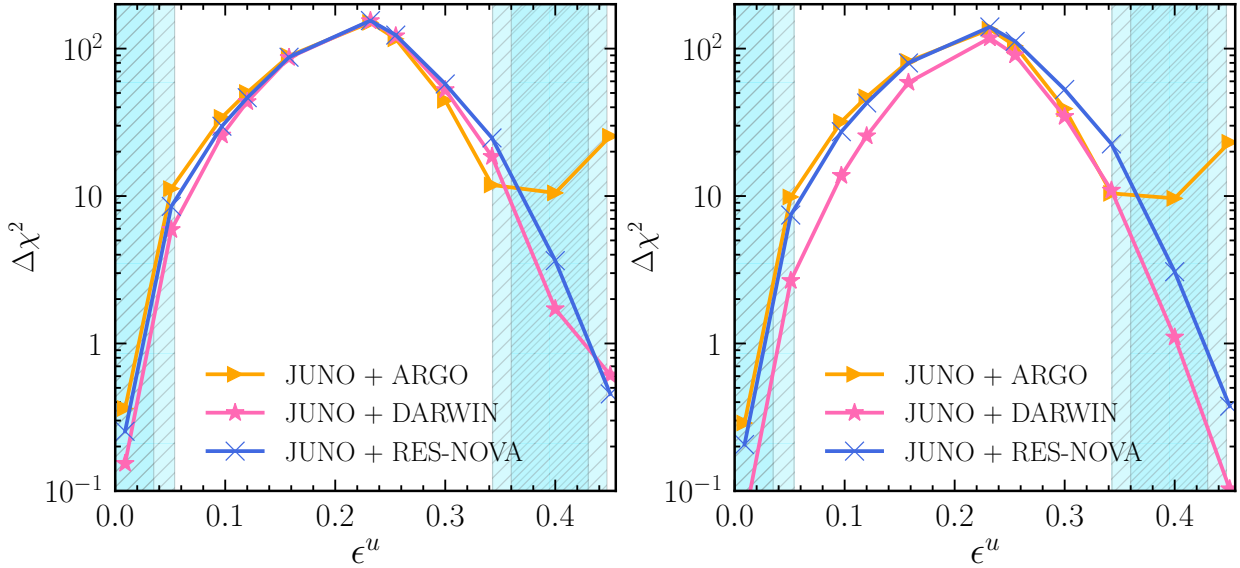


Figure 7. *Left Panel:* Same as Figure 3, but with increased uncertainties $\sigma_x = 25\%$, $\sigma_y = 20\%$, and $\sigma_z = 20\%$. *Right Panel:* Same as the *left panel* but the distance to the supernova $D = 1$ kpc.

Figure 7 depicts the results of our statistical analysis for three different cases: (i) the SN neutrino flux and cross section uncertainties are increased to $\sigma_x = 25\%$, $\sigma_y = 20\%$, and $\sigma_z = 20\%$ with respect to Figure 3 (left panel) and (ii) the uncertainties are large and the distance to the SN is increased to $D = 1$ kpc compared to Figure 3. The increase in the uncertainty or distance to the SN does not change our results significantly.

REFERENCES

Aalbers, J., et al. 2016, JCAP, 11, 017,
doi: [10.1088/1475-7516/2016/11/017](https://doi.org/10.1088/1475-7516/2016/11/017)
—. 2024. <https://arxiv.org/abs/2410.17137>

Aalseth, C. E., et al. 2018, Eur. Phys. J. Plus, 133, 131,
doi: [10.1140/epjp/i2018-11973-4](https://doi.org/10.1140/epjp/i2018-11973-4)

- Abe, K., et al. 2017, *Astropart. Phys.*, 89, 51, doi: [10.1016/j.astropartphys.2017.01.006](https://doi.org/10.1016/j.astropartphys.2017.01.006)
- . 2022, *Nucl. Instrum. Meth. A*, 1027, 166248, doi: [10.1016/j.nima.2021.166248](https://doi.org/10.1016/j.nima.2021.166248)
- Abe, S., et al. 2024, *Astrophys. J.*, 973, 140, doi: [10.3847/1538-4357/ad5fee](https://doi.org/10.3847/1538-4357/ad5fee)
- Abi, B., et al. 2021, *Eur. Phys. J. C*, 81, 423, doi: [10.1140/epjc/s10052-021-09166-w](https://doi.org/10.1140/epjc/s10052-021-09166-w)
- Adamski, S., et al. 2025, *Phys. Rev. Lett.*, 134, 231801, doi: [10.1103/PhysRevLett.134.231801](https://doi.org/10.1103/PhysRevLett.134.231801)
- Ahmad, Q. R., et al. 2002, *Phys. Rev. Lett.*, 89, 011301, doi: [10.1103/PhysRevLett.89.011301](https://doi.org/10.1103/PhysRevLett.89.011301)
- Akimov, D., et al. 2017, *Science*, 357, 1123, doi: [10.1126/science.aao0990](https://doi.org/10.1126/science.aao0990)
- . 2021, *Phys. Rev. Lett.*, 126, 012002, doi: [10.1103/PhysRevLett.126.012002](https://doi.org/10.1103/PhysRevLett.126.012002)
- Alexeyev, E., Alexeyeva, L., Krivosheina, I., & Volchenko, V. 1988, *Physics Letters B*, 205, 209, doi: [https://doi.org/10.1016/0370-2693\(88\)91651-6](https://doi.org/10.1016/0370-2693(88)91651-6)
- An, F., et al. 2016, *J. Phys. G*, 43, 030401, doi: [10.1088/0954-3899/43/3/030401](https://doi.org/10.1088/0954-3899/43/3/030401)
- Aprile, E., et al. 2018, *Phys. Rev. Lett.*, 121, 111302, doi: [10.1103/PhysRevLett.121.111302](https://doi.org/10.1103/PhysRevLett.121.111302)
- . 2021, *Phys. Rev. Lett.*, 126, 091301, doi: [10.1103/PhysRevLett.126.091301](https://doi.org/10.1103/PhysRevLett.126.091301)
- . 2024, *Phys. Rev. Lett.*, 133, 191002, doi: [10.1103/PhysRevLett.133.191002](https://doi.org/10.1103/PhysRevLett.133.191002)
- Aristizabal Sierra, D., Dutta, B., Liao, S., & Strigari, L. E. 2019, *JHEP*, 12, 124, doi: [10.1007/JHEP12\(2019\)124](https://doi.org/10.1007/JHEP12(2019)124)
- Aristizabal Sierra, D., Mishra, N., & Strigari, L. 2025, *Phys. Rev. D*, 111, 055007, doi: [10.1103/PhysRevD.111.055007](https://doi.org/10.1103/PhysRevD.111.055007)
- Beacom, J. F., Farr, W. M., & Vogel, P. 2002, *Phys. Rev. D*, 66, 033001, doi: [10.1103/PhysRevD.66.033001](https://doi.org/10.1103/PhysRevD.66.033001)
- Beeman, J. W., et al. 2022, *Eur. Phys. J. C*, 82, 692, doi: [10.1140/epjc/s10052-022-10656-8](https://doi.org/10.1140/epjc/s10052-022-10656-8)
- Bionta, R. M., et al. 1987, *Phys. Rev. Lett.*, 58, 1494, doi: [10.1103/PhysRevLett.58.1494](https://doi.org/10.1103/PhysRevLett.58.1494)
- Blanco-Mas, P., Coloma, P., Herrera, G., et al. 2025, *JHEP*, 08, 043, doi: [10.1007/JHEP08\(2025\)043](https://doi.org/10.1007/JHEP08(2025)043)
- Blennow, M., Mirizzi, A., & Serpico, P. D. 2008, *Phys. Rev. D*, 78, 113004, doi: [10.1103/PhysRevD.78.113004](https://doi.org/10.1103/PhysRevD.78.113004)
- Bo, Z., et al. 2024, *Phys. Rev. Lett.*, 133, 191001, doi: [10.1103/PhysRevLett.133.191001](https://doi.org/10.1103/PhysRevLett.133.191001)
- Boehm, C., Cerdeño, D. G., Machado, P. A. N., et al. 2019, *JCAP*, 01, 043, doi: [10.1088/1475-7516/2019/01/043](https://doi.org/10.1088/1475-7516/2019/01/043)
- Bonet, H., et al. 2022, *JHEP*, 05, 085, doi: [10.1007/JHEP05\(2022\)085](https://doi.org/10.1007/JHEP05(2022)085)
- Cerdeño, D. G., Cermeño, M., & Farzan, Y. 2023, *Phys. Rev. D*, 107, 123012, doi: [10.1103/PhysRevD.107.123012](https://doi.org/10.1103/PhysRevD.107.123012)
- Cerdeño, D. G., Cermeño, M., Pérez-García, M. Á., & Reid, E. 2021, *Phys. Rev. D*, 104, 063013, doi: [10.1103/PhysRevD.104.063013](https://doi.org/10.1103/PhysRevD.104.063013)
- Cerdeño, D. G., Fairbairn, M., Jubb, T., et al. 2016, *JHEP*, 05, 118, doi: [10.1007/JHEP09\(2016\)048](https://doi.org/10.1007/JHEP09(2016)048)
- Chauhan, B., Dasgupta, B., & Dighe, A. 2022, *Phys. Rev. D*, 105, 095035, doi: [10.1103/PhysRevD.105.095035](https://doi.org/10.1103/PhysRevD.105.095035)
- Coloma, P., Esteban, I., Gonzalez-Garcia, M. C., et al. 2022, *JHEP*, 05, 037, doi: [10.1007/JHEP05\(2022\)037](https://doi.org/10.1007/JHEP05(2022)037)
- Dasgupta, B., & Beacom, J. F. 2011, *Phys. Rev. D*, 83, 113006, doi: [10.1103/PhysRevD.83.113006](https://doi.org/10.1103/PhysRevD.83.113006)
- De Romeri, V., Miranda, O. G., Papoulias, D. K., et al. 2023, *JHEP*, 04, 035, doi: [10.1007/JHEP04\(2023\)035](https://doi.org/10.1007/JHEP04(2023)035)
- De Romeri, V., Papoulias, D. K., & Ternes, C. A. 2025, *JCAP*, 05, 012, doi: [10.1088/1475-7516/2025/05/012](https://doi.org/10.1088/1475-7516/2025/05/012)
- Dev, P. S. B., et al. 2019, 2, 001, doi: [10.21468/SciPostPhysProc.2.001](https://doi.org/10.21468/SciPostPhysProc.2.001)
- Duan, H., Fuller, G. M., & Qian, Y.-Z. 2010, *Ann. Rev. Nucl. Part. Sci.*, 60, 569, doi: [10.1146/annurev.nucl.012809.104524](https://doi.org/10.1146/annurev.nucl.012809.104524)
- Dutta, B., Karthikeyan, A., Mishra, N., Porto, Y., & Strigari, L. E. 2025. <https://arxiv.org/abs/2508.16558>
- Esteban-Pretel, A., Tomas, R., & Valle, J. W. F. 2010, *Phys. Rev. D*, 81, 063003, doi: [10.1103/PhysRevD.81.063003](https://doi.org/10.1103/PhysRevD.81.063003)
- Farzan, Y., Lindner, M., Rodejohann, W., & Xu, X.-J. 2018, *JHEP*, 05, 066, doi: [10.1007/JHEP05\(2018\)066](https://doi.org/10.1007/JHEP05(2018)066)
- Fogli, G. L., Lisi, E., Mirizzi, A., & Montanino, D. 2002, *Phys. Rev. D*, 66, 013009, doi: [10.1103/PhysRevD.66.013009](https://doi.org/10.1103/PhysRevD.66.013009)
- Freedman, D. Z. 1974, *Phys. Rev. D*, 9, 1389, doi: [10.1103/PhysRevD.9.1389](https://doi.org/10.1103/PhysRevD.9.1389)
- Fukuda, Y., et al. 1998, *Phys. Rev. Lett.*, 81, 1562, doi: [10.1103/PhysRevLett.81.1562](https://doi.org/10.1103/PhysRevLett.81.1562)
- Gehrlein, J., & Kushwaha, T. 2025. <https://arxiv.org/abs/2508.14166>
- Harnik, R., Kopp, J., & Machado, P. A. N. 2012, *JCAP*, 07, 026, doi: [10.1088/1475-7516/2012/07/026](https://doi.org/10.1088/1475-7516/2012/07/026)
- Helm, R. H. 1956, *Phys. Rev.*, 104, 1466, doi: [10.1103/PhysRev.104.1466](https://doi.org/10.1103/PhysRev.104.1466)
- Hirata, K., Kajita, T., Koshiba, M., et al. 1987, *Phys. Rev. Lett.*, 58, 1490, doi: [10.1103/PhysRevLett.58.1490](https://doi.org/10.1103/PhysRevLett.58.1490)
- Huang, X.-R., Zha, S., & Chen, L.-W. 2021, *Astrophys. J. Lett.*, 923, L26, doi: [10.3847/2041-8213/ac4014](https://doi.org/10.3847/2041-8213/ac4014)
- Joyce, M., Leung, S.-C., Molnár, L., et al. 2020, *The Astrophysical Journal*, 902, 63, doi: [10.3847/1538-4357/abb8db](https://doi.org/10.3847/1538-4357/abb8db)
- Keil, M. T., Raffelt, G. G., & Janka, H.-T. 2003, *Astrophys. J.*, 590, 971, doi: [10.1086/375130](https://doi.org/10.1086/375130)
- Khaitan, D. 2018, *JINST*, 13, C02024, doi: [10.1088/1748-0221/13/02/C02024](https://doi.org/10.1088/1748-0221/13/02/C02024)
- Kozyneets, T., Fallows, S., & Krauss, C. B. 2019, *Astropart. Phys.*, 105, 25, doi: [10.1016/j.astropartphys.2018.09.004](https://doi.org/10.1016/j.astropartphys.2018.09.004)

- Lang, R. F., McCabe, C., Reichard, S., Selvi, M., & Tamborra, I. 2016, Phys. Rev. D, 94, 103009, doi: [10.1103/PhysRevD.94.103009](https://doi.org/10.1103/PhysRevD.94.103009)
- Langanke, K., Vogel, P., & Kolbe, E. 1996, Phys. Rev. Lett., 76, 2629, doi: [10.1103/PhysRevLett.76.2629](https://doi.org/10.1103/PhysRevLett.76.2629)
- Lattimer, J. M., & Swesty, F. D. 1991, Nucl. Phys. A, 535, 331, doi: [10.1016/0375-9474\(91\)90452-C](https://doi.org/10.1016/0375-9474(91)90452-C)
- Lei, M., Steinberg, N., & Wells, J. D. 2020, JHEP, 01, 179, doi: [10.1007/JHEP01\(2020\)179](https://doi.org/10.1007/JHEP01(2020)179)
- Li, G., Song, C.-Q., Tang, F.-J., & Yu, J.-H. 2025, Phys. Rev. D, 111, 035002, doi: [10.1103/PhysRevD.111.035002](https://doi.org/10.1103/PhysRevD.111.035002)
- Liao, J., Marfatia, D., & Zhang, J. 2024, Phys. Rev. D, 110, 055040, doi: [10.1103/PhysRevD.110.055040](https://doi.org/10.1103/PhysRevD.110.055040)
- Lu, J.-S., Li, Y.-F., & Zhou, S. 2016, Phys. Rev. D, 94, 023006, doi: [10.1103/PhysRevD.94.023006](https://doi.org/10.1103/PhysRevD.94.023006)
- Maity, T. N., & Boehm, C. 2025, Phys. Rev. D, 112, 053001, doi: [10.1103/11gl-bx7v](https://doi.org/10.1103/11gl-bx7v)
- Mansour, S., & Kuo, T.-K. 1998, Phys. Rev. D, 58, 013012, doi: [10.1103/PhysRevD.58.013012](https://doi.org/10.1103/PhysRevD.58.013012)
- Mikheev, S. P., & Smirnov, A. Y. 1986, Sov. Phys. JETP, 64, 4. <https://arxiv.org/abs/0706.0454>
- Mikheyev, S. P., & Smirnov, A. Y. 1985, Sov. J. Nucl. Phys., 42, 913
- Mukhopadhyay, M., Lunardini, C., Timmes, F. X., & Zuber, K. 2020, Astrophys. J., 899, 153, doi: [10.3847/1538-4357/ab99a6](https://doi.org/10.3847/1538-4357/ab99a6)
- Newmark, D. A., & Schneider, A. 2023, Phys. Rev. D, 108, 043005, doi: [10.1103/PhysRevD.108.043005](https://doi.org/10.1103/PhysRevD.108.043005)
- Nunokawa, H., Qian, Y. Z., Rossi, A., & Valle, J. W. F. 1996, Phys. Rev. D, 54, 4356, doi: [10.1103/PhysRevD.54.4356](https://doi.org/10.1103/PhysRevD.54.4356)
- O'Connor, E. 2015, Astrophys. J. Suppl., 219, 24, doi: [10.1088/0067-0049/219/2/24](https://doi.org/10.1088/0067-0049/219/2/24)
- O'Connor, E., & Ott, C. D. 2010, Class. Quant. Grav., 27, 114103, doi: [10.1088/0264-9381/27/11/114103](https://doi.org/10.1088/0264-9381/27/11/114103)
- Pattavina, L., Ferreiro Iachellini, N., & Tamborra, I. 2020, Phys. Rev. D, 102, 063001, doi: [10.1103/PhysRevD.102.063001](https://doi.org/10.1103/PhysRevD.102.063001)
- Raj, N., Takhistov, V., & Witte, S. J. 2020, Phys. Rev. D, 101, 043008, doi: [10.1103/PhysRevD.101.043008](https://doi.org/10.1103/PhysRevD.101.043008)
- Schwemberger, T., Takhistov, V., & Yu, T.-T. 2024, JCAP, 11, 068, doi: [10.1088/1475-7516/2024/11/068](https://doi.org/10.1088/1475-7516/2024/11/068)
- Schwemberger, T., & Yu, T.-T. 2022, Phys. Rev. D, 106, 015002, doi: [10.1103/PhysRevD.106.015002](https://doi.org/10.1103/PhysRevD.106.015002)
- Stapleford, C. J., Väänänen, D. J., Kneller, J. P., McLaughlin, G. C., & Shapiro, B. T. 2016, Phys. Rev. D, 94, 093007, doi: [10.1103/PhysRevD.94.093007](https://doi.org/10.1103/PhysRevD.94.093007)
- Suliga, A. M., & Tamborra, I. 2021, Phys. Rev. D, 103, 083002, doi: [10.1103/PhysRevD.103.083002](https://doi.org/10.1103/PhysRevD.103.083002)
- Sullivan, C., O'Connor, E., Zegers, R. G. T., Grubb, T., & Austin, S. M. 2016, Astrophys. J., 816, 44, doi: [10.3847/0004-637X/816/1/44](https://doi.org/10.3847/0004-637X/816/1/44)
- Tamborra, I., & Shalgar, S. 2021, Ann. Rev. Nucl. Part. Sci., 71, 165, doi: [10.1146/annurev-nucl-102920-050505](https://doi.org/10.1146/annurev-nucl-102920-050505)
- Tornow, W., Tonchev, A. P., Finch, S. W., et al. 2022, Phys. Lett. B, 835, 137576, doi: [10.1016/j.physletb.2022.137576](https://doi.org/10.1016/j.physletb.2022.137576)
- Valle, J. W. F. 1987, Phys. Lett. B, 199, 432, doi: [10.1016/0370-2693\(87\)90947-6](https://doi.org/10.1016/0370-2693(87)90947-6)
- Volpe, M. C. 2023. <https://arxiv.org/abs/2301.11814>
- Weatherly, P., et al. 2022. <https://arxiv.org/abs/2203.11772>
- Wolfenstein, L. 1978, Phys. Rev. D, 17, 2369, doi: [10.1103/PhysRevD.17.2369](https://doi.org/10.1103/PhysRevD.17.2369)
- Woosley, S. E., & Weaver, T. A. 1995, Astrophys. J. Suppl., 101, 181, doi: [10.1086/192237](https://doi.org/10.1086/192237)
- Workman, R. L., et al. 2022, PTEP, 2022, 083C01, doi: [10.1093/ptep/ptac097](https://doi.org/10.1093/ptep/ptac097)